

Preparation of a Highly-Efficient Electro-Fenton Cathode Material for H₂O₂ Generation and Its Electrochemical Performance in COD Removal

Hongli Zhang¹, Zeyu Xu², Shaoliang Wang², Xinzhuang Fan^{1,2,*}

¹ Guangzhou HKUST Fok Ying Tung Research Institute, Guangzhou, China;

² Institute of Metal Research, Chinese Academy of Sciences, Shenyang, China.

*E-mail: mexzfan@gmail.com

Received: 25 July 2020 / Accepted: 19 September 2020 / Published: 31 October 2020

As a typical cathode material for electro-Fenton, the surface active compositions and pore structure of the polyacrylonitrile-based carbon fibers (PAN-CFs) are important to ensure the electrochemical activity of oxygen reduction reaction (ORR) and the corresponding electro-Fenton efficiency. In order to further improve the electro-generating efficiency of H₂O₂, PAN-based carbon nanofibers (PAN-CNFs) with high surface area, good conductivity and excellent electrochemical activity were prepared through the electrospinning, as well as the following graphitization and activation treatment. Results show that the as-prepared NH₃ modified PAN-CNFs (N-PAN-CNFs) have high selectivity and good electrochemical stability for the two-electron ORR in the acidic solution, and it is worth noting that the electro-generating efficiency of H₂O₂ is high up to 98%. In addition, the electrocatalytic oxidation of phenol solution with the concentration of 100 mg L⁻¹ is investigated with N-PAN-CNFs as the cathode material of electro-Fenton. It is found that the *COD_{Cr}* and average current efficiency after the electro-Fenton treatment for 3 h are high up to 85% and 80% respectively, while the corresponding energy consumption is just 25.6 kWh kg⁻¹ COD. The excellent electrochemical performance of N-PAN-CNFs might be ascribed to the reasonable pore structure, high surface area (89.7 m² g⁻¹), good conductivity (93.7 S cm⁻¹) and abundant graphitic-N and pyrrolic-N (high up to 62%). Therefore, N-PAN-CNFs are expected to be widely used as efficient cathode materials for the electro-Fenton in the sewage treatment.

Keywords: Electrospinning; Electro-Fenton; Oxygen reduction reaction; Pore structure; Nitrogen functional groups.

1. INTRODUCTION

With the rapid development of the chemical industries such as the petrochemical fiber, papermaking, dyeing, as well as the rubber and plastics, the industrial wastewater containing large amounts of hazardous residue has increased simultaneously, resulting in serious pollution to the

environment. The People who are committed to protect the environment have made various attempts to search for an efficient and economical treatment of such wastewater, and also proposed many treatment methods. However, for the wastewater containing some organic pollutants which are difficult to biodegrade, such as the polycyclic aromatic hydrocarbons, halogenated hydrocarbons, heterocyclic compounds and organic dyes, it is still hard to meet the emission standards even with the conventional physical, chemical and biological treatments, or else the corresponding treatment cost is extremely high. Both of these issues make the treatment of such difficultly biodegradable organic wastewater a research hotspot [1]. Fenton oxidation is a typical oxidation technology that can efficiently generate strong oxidizing hydroxyl radicals, but it still has some disadvantages such as the low utilization of H_2O_2 , rapid decay of oxidation efficiency, difficulty in regeneration of Fe^{2+} , and large amount of sludge [1-3]. In order to overcome the above-mentioned shortcomings, some auxiliary methods such as light, electricity, ultrasound, microwave, etc. are introduced into the Fenton oxidation system. Among them, the electro-Fenton technology, in which the Fenton reagent is partially or completely generated in situ by the electrochemical methods, exhibits the advantages of in-situ generated H_2O_2 , regenerated Fe^{2+} at the cathode, and less sludge [4].

During the cathodic process of the electro-Fenton system, H_2O_2 is generated through a two-electron reduction reaction of the dissolved oxygen at the surface of cathode, so the cathode materials with high activity of the two-electron oxygen reduction reaction (ORR) play an important role in ensuring an efficient electro-Fenton reaction. However, the commercial electro-Fenton cathodes still have the disadvantages of poor mass transfer, low oxygen utilization, low current efficiency of electro-generating H_2O_2 , and high energy consumption. In addition, there are still few studies on the relationship between the oxygen reduction performance and physico-chemical properties of the cathode materials till now. Therefore, there is an urgent need to focus on the research of the electro-Fenton cathode materials.

Among many cathode materials that can be used in the electro-Fenton system, carbon materials have been widely used in the research on the H_2O_2 generation through ORR as early as the 1970s, due to their good electrical conductivity, high corrosion resistance, favorable chemical stability and high hydrogen evolution potential. Up to now, the reported carbon materials used in the electro-Fenton process are mainly graphite, activated carbon fibers (ACFs), carbon nanotubes (CNTs), reticulated glassy carbon (RGC), carbon sponges (CSs) and graphite felts (GFs) [5]. Specifically, the ACFs and GFs that possess a higher surface area often exhibit a greater cumulative amount of electro-generated H_2O_2 . Despite of the large cumulative amount of H_2O_2 generated at GFs, the corresponding electro-generating efficiency of H_2O_2 is a little small, resulting in an unsatisfied electrochemical performance for ORR [5]. Therefore, some researchers have tried to improve the electrocatalytic activity of ORR through the post-treatment of GFs. For instance, Miao and his co-workers modified the GFs through the electrochemical anodization in H_2SO_4 solution. They found that the cumulative concentration of H_2O_2 at the surface of GFs was more than 6 times of that for the pristine GFs, and the electro-generating efficiency of H_2O_2 was significantly improved, which might be attributed to the rougher surface and rich oxygen-containing groups for the modified GFs [6]. Zhou et al. once used the low-cost ethanol and hydrazine-modified GFs as the cathode for the electro-Fenton process to degrade the p-nitrophenol in the wastewater [7], and it was found that a large number of carbon nanoparticles were generated at the surface of the modified GFs, meanwhile the oxygen-containing and nitrogen-containing functional

groups also significantly increased, both of which greatly improve the electrode's hydrophilicity and electrocatalytic activity of ORR, further enhancing the degradation rate of p-nitrophenol [7]. The above-mentioned results show that the increase of surface functional groups during the traditional modification process is often accompanied with the increase in the surface area, so the synergy effect of the increase in the active component and surface area leads to a significant increase in the efficiency of the electro-generated H_2O_2 . In fact, the specific surface area of the commercial GFs is only $0.05\text{-}0.5\text{ m}^2\text{ g}^{-1}$ [8, 9], while that of other porous carbon materials are hundreds or even thousands of square meters per gram. Therefore, the enhancement of the surface area may be more meaningful for the improvement of the electro-generated H_2O_2 performance for GFs.

Generally, the two-electron ORR are more expected in the electro-Fenton system, so we need the active component on the electrode surface to have excellent selectivity for the two-electron ORR, and the nitrogen-containing groups often behave a better selectivity than oxygen-containing groups. Lee et al. [10] synthesized the collagen-crosslinked paraformaldehyde by vacuum heating at different temperatures to obtain the nitrogen-doped carbon with a high porosity. It was found that the as-prepared carbon sample heated at $400\text{-}800\text{ }^\circ\text{C}$ for 4 h has a high selectivity to the two-electron ORR, and the electro-generation efficiency of H_2O_2 can be as high as 93%, which is mainly due to the synergy effect between the nitrogen-doped structure and oxygen-containing functional group on the surface of the carbon material, further resulting in its high selectivity for the formation of H_2O_2 . Zhang et al. [11] used nitrogen-functionalized multi-walled CNTs (N-CNTs) as the cathode material of the electro-Fenton system. They found that the presence of nitrogen functional groups accelerates the two-electron ORR process, and therefore its electro-generated H_2O_2 performance is significantly improved. In addition, such material can quickly remove methyl orange when it is used to degrade methyl orange in electro-Fenton system. Xu et al. [12] found that the intrinsic pyridine nitrogen structure of PAN-based carbon fibers (PAN-CFs) was converted to 2-pyridone during the electrochemical modification, forming the N and O co-modified ORR active functional groups. More importantly, the N and O co-linked C, which has a higher positive charge density, becomes the dominant active site, exhibiting the preferable activity and selectivity to catalyze the two-electron ORR in acidic and alkaline solutions. Therefore, the introduction of the nitrogen-containing functional groups is conducive to the two-electron ORR, further improving the electro-generating efficiency of H_2O_2 .

Electrospinning technology is one of the simplest and most effective methods to obtain nanofibers by far, and carbon fibers with different target characteristics can be easily prepared by adding functional groups into the spinning solution. Hence, the electrospinning carbon nanofibers have already been used as the electrodes in supercapacitors [13], lithium batteries [14], vanadium flow batteries [15, 16] and other fields. In order to obtain an electro-Fenton cathode material with suitable pore structure, higher specific surface, electrical conductivity and electrochemical activity, we intend to prepare the PAN-based carbon nanofibers (PAN-CNFs) by the electrospinning technology, combined with subsequent graphitization and activation treatments in this work. Among them, the graphitization treatment can improve the conductivity of the electrode, and the activation treatment will not only improve the selectivity of the two-electron ORR, but also further optimize the pore structure of the electrode, which will result in a remarkable increase in the mesopores proportion and specific surface area, further improving the mass transfer at the surface of the electrode.

2. EXPERIMENTAL

2.1. Reagents and instruments

The PAN powder with an average molecular weight of 90,000 was purchased from Kunshan Hongyu Plastic Co., Ltd., and other reagents such as dimethylformamide (DMF), phenol, potassium titanium oxalate, sodium sulfate, ferrous sulfate heptahydrate, sulfuric acid, ethanol were purchased from Sinopharm Reagent Co., Ltd. All the reagents are analytical grade, and the deionized water used in this work is made by the laboratory.

The electrospinning machine with the model of KH-2 was purchased from Jinan Liangrui Technology Co., Ltd. The graphitization furnace and activation furnace are YVG-2020I C and YQFS-1700, which were produced by Shanghai Yuzhi Mechanical and Electrical Equipment Co., Ltd. The potentiostat of CHI-700E purchased from Shanghai Chenhua Instrument Co., Ltd. along with the MSR rotating disk electrode system produced by Pine together constituted a set of electrochemical testing system. In addition, the UV-Vis spectrophotometer of UV 2450 was produced by SHIMADZU in Japan, and the Delta 320 pH meter was purchased from Mettler Toledo.

2.2. Preparation of the electrodes

Firstly, we dissolved the PAN powder in DMF (12 wt.%) and kept the suspension magnetic stirring at 60 °C for 4 hours, then used a syringe to draw 10 mL of the spinning solution for electrospinning. Herein, a syringe needle with a diameter of 0.6 mm was used as the electrospinning nozzle, and a piece of aluminum foil was served as the collector. During the spinning process, the voltage between the needle and collector is 20 kV, meanwhile the distance between them is 10 cm. In addition, the speed of the roller is 500 r min⁻¹, and the spinning temperature and humidity are 25 °C and 40%RH respectively. Secondly, the above-prepared electrospun nanofibers were pre-oxidized in air at 280 °C for 1 h according to the previous post-processing technology [17,18], and then carbonized at 1000 °C for 2 h under the protection of argon to obtain PAN-CNFs. Thirdly, we put the PAN-CNFs in an argon atmosphere at 2300 °C for 2 h to conduct the graphitization treatment, and then placed them in the NH₃ atmosphere at 800 °C for 1 h to complete the activation treatment, in which the NH₃ flow rate was 50 sccm. After the incubation, the samples were cooled to room temperature in the NH₃ atmosphere, and the samples were taken out and labeled as N-PAN-CNFs.

2.3. Physico-chemical characterizations

Scanning electron microscope (SEM, XL30FEG, Philips) was used to observe the surface morphology of the samples. ASAP 2020 adsorption (Micromeritics, USA) was used under the liquid nitrogen atmosphere (77 K) for the BET test. In addition, 4 Probe tester (RTS8, Guangzhou 4 Probe Technology Co., Ltd.) was used to measure the conductivity of the electrode, and X-ray photoelectron spectroscopy (XPS, ESCALAB250, VG) was used to analyze the element content at the surface of the samples.

2.4. Electrochemical measurements

The samples of PAN-CNFs and N-PAN-CNFs were used as the working electrode (1 cm²), a DSA mesh (9 cm²) and a saturated calomel electrode (SCE) were used as the auxiliary electrode and reference electrode for the electro-generating H₂O₂ tests. In order to reduce the liquid junction potential and avoid contamination of the reference electrode, a salt bridge was used to connect the reference electrode and electrolyte. All voltage values in the work are relative to SCE.

The electro-generating H₂O₂ tests were carried out in the above-mentioned three-electrode system, the blended H₂SO₄+Na₂SO₄ solution with a pH of 3 was used as the electrolyte. Herein, the Na₂SO₄ solution with the concentration of 0.1 mol L⁻¹ was used as the supporting electrolyte, and the overall volume of the electrolyte was 0.5 L. The electrolysis with a constant current of 100 mA was conducted with the CHI700E potentiostat, and a certain amount of electrolyte is taken out from the electrolytic cell every 25 mins. After filtering the electrolyte sample, the UV spectrum was recorded with a UV2450 spectrophotometer. In addition, the cumulative concentration of H₂O₂ can be determined by the visible absorption of the colored complex of Ti (IV) at a wavelength of 400 nm [19], and the following formula was used in this paper [20]:

$$C_{H_2O_2} = 1.53802 + 204.43687A \quad (1)$$

Where $C_{H_2O_2}$ is the concentration of H₂O₂ in the electrolyte (mg L⁻¹), and A is the absorbance.

In addition, the current efficiency of the electro-generating H₂O₂ can be calculated by the following formula [21]:

$$CE = \frac{zFC_{H_2O_2}V}{M_{H_2O_2}It} \times 100\% \quad (2)$$

Where CE refers to the current efficiency (%), z is the number of electrons transferred during the ORR from O₂ to H₂O₂, F is the Faraday constant (96485 C mol⁻¹), V is the solution volume (L), $M_{H_2O_2}$ is the molar mass of H₂O₂ (34.01 g mol⁻¹), I is the electrolysis current (A), t is the electrolysis time (s).

In order to evaluate the ORR activity of the samples, we used the CHI700E potentiostat combined with the MSR rotating disk electrode system to test the cyclic voltammetry (CV) behavior of the two electrodes, and conducted the linear sweep voltammetry (LSV) tests through adjusting the rotating speed of the electrode. In addition, oxygen gas was supplied for about 10 mins before the electrochemical test to ensure that the electrolyte was saturated with oxygen.

Furthermore, the experiment of electro-Fenton degradation of phenol was carried out in a two-electrode system composed of a DSA mesh anode and a N-PAN-CNFs cathode. The electrolyte (0.5 L) with the pH value of 3 is composed of H₂SO₄, FeSO₄ and Na₂SO₄. Herein, Na₂SO₄ with the concentration of 0.1 mol L⁻¹ is the supporting electrolyte, and the concentration of Fe²⁺ and phenol in the electrolyte is 0.3 mol L⁻¹ and 100 mg L⁻¹ respectively. The constant current mode was adopted during the electrolysis process. Specifically, the electrolysis current is 100 mA, and the electrolysis time is 30, 60, 90, 120, 150, 180, 210 and 240 min, respectively. After filtering the electrolyzed solution, the ultraviolet spectrum was recorded with a UV 2450 spectrophotometer. The degradation effect of phenol was evaluated by the change of ultraviolet spectrum and the corresponding COD_{Cr} removal rate. The COD_{Cr} was measured by standard method of HJ-T 399-2007 [1], the specific formula is as follows:

$$COD_{Cr} = \frac{COD_0 - COD_t}{COD_0} \times 100\% \quad (3)$$

Where COD_{Cr} refers to the color removal rate of the solution, COD_0 refers to the initial COD of the solution, and COD_t is the COD of the solution after t min.

In addition, the average current efficiency (ACE) and electrochemical energy consumption (EEC) of phenol mineralization are calculated by equation (4) and (5) respectively [1]:

$$ACE = \frac{(COD_0 - COD_t) \times F \times V}{8 \times I \times t} \times 100\% \quad (4)$$

$$EEC = \frac{U \times I \times t}{(COD_0 - COD_t) \times V} \times 100\% \quad (5)$$

Where ACE and EEC are average current efficiency and electrochemical energy consumption respectively, the constant of 8 is the oxygen equivalent mass ($g \text{ eq}^{-1}$), U is the electrolysis voltage (V), and other parameters are the same as described above.

3. RESULTS AND DISCUSSION

3.1. Physico-chemical characterizations

Firstly, the effects of the graphitization treatment combined with the ammonia activation treatment on the surface morphology of the carbon nanofibers were investigated. As shown in Fig. 1, the fiber diameter of both PAN-CNFs and N-PAN-CNFs are about 200 nm, meanwhile the latter is slightly less than the former. This is because that the electrospun nanofibers are carbonized at the carbonization temperature ($1000 \text{ }^\circ\text{C}$), at this time most of the unstable polymers and solvents in the carbon fibers are almost completely decomposed, resulting in a relatively stable basic skeleton, so the graphitization treatment ($2300 \text{ }^\circ\text{C}$) and following activation treatment has little effect on the fiber diameter. However, compared with PAN-CNFs (Fig. 1(a)), there are less particles can be observed at the surface of N-PAN-CNFs, but more ravines are formed at the surface (Fig. 1(b)). This is mainly due to that the particles on the fiber surface are basically completely decomposed at a temperature of $2300 \text{ }^\circ\text{C}$, meanwhile some unstable components in the surface layer of the fiber will continue to decompose. Furthermore, the attacks by the ammonia molecules during the activation treatment will lead to the decomposition of the unstable components in the surface layer of the fiber as well, and both these two aspects result in the formation of surface ravines, which is undoubtedly beneficial to increase the surface area of N-PAN-CNFs.

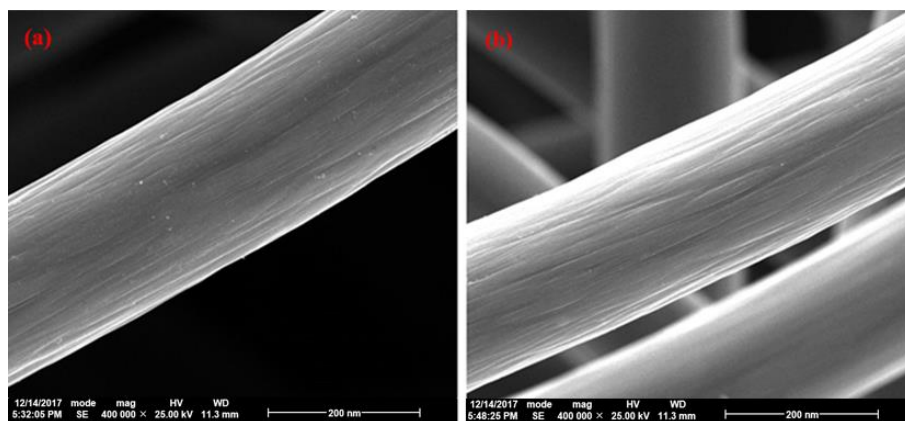


Figure 1. SEM images of PAN-CNFs (a) and N-PAN-CNFs (b)

In order to verify the above viewpoint, we conducted the BET test for PAN-CNFs and N-PAN-CNFs. It is found that the specific surface area of PAN-CNFs is $53.6 \text{ m}^2 \text{ g}^{-1}$, while that of N-PAN-CNFs is $89.7 \text{ m}^2 \text{ g}^{-1}$. There is no doubt that the improvement of the specific surface of N-PAN-CNFs is due to the ravines at the surface of the carbon fiber (Fig. 1(b)). Fig. 2 shows the pore size distribution of PAN-CNFs and N-PAN-CNFs. Through the comparison, it is found that the pores of PAN-CNFs are mainly micropores of about 2 nm and mesopores of about 5 nm, while those of N-PAN-CNFs are mainly mesopores about 4.5 and 7 nm. Definitely, more mesopores are obviously more conducive to the mass transfer process of electroactive substances [22]. In addition, although the presence of micropores is conducive to the increase of the specific surface area, the proportion of micropores in PAN-CNFs is relatively small, so the contribution of the micropores in PAN-CNFs to the specific surface area is quite limited. While the proportion of mesopores (especially the mesopores around 7 nm) in N-PAN-CNFs is significantly larger than that of the former, so they can provide more surface area. Therefore, the overall specific surface area of N-PAN-CNFs increased by 67% compared with that of PAN-CNFs. In short, N-PAN-CNFs have a more optimized pore structure and higher surface area, both of which are beneficial to the improvement of the performance of electro-generating H_2O_2 .

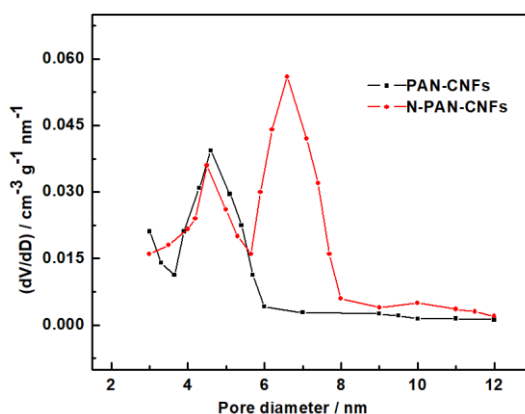


Figure 2. Pore size distribution curves of PAN-CNFs and N-PAN-CNFs

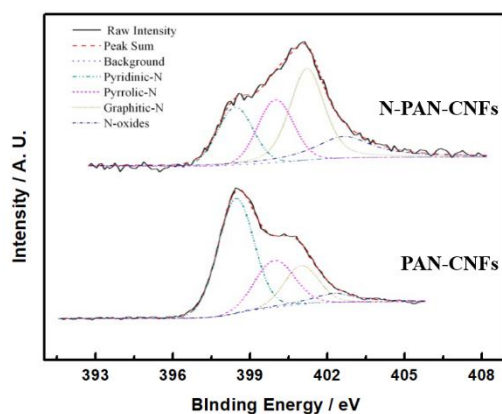


Figure 3. Curve-fitting of the N1s high-resolution XPS from the PAN-CNFs and N-PAN-CNFs

Table 1. Elements and corresponding content of PAN-CNFs and N-PAN-CNFs

Samples	C	O	N
PAN-CNFs	92.92	3.10	3.98
N-PAN-CNFs	91.30	1.08	7.62

Subsequently, in order to investigate the active components at the surface of carbon fiber, we performed the XPS analysis on PAN-CNFs and N-PAN-CNFs. As shown in Table 1, although the main elements of PAN-CNFs and N-PAN-CNFs are C, N, O, and the carbon content of these two samples have little different, the oxygen content of the former is relatively close to the nitrogen content, while the nitrogen content of the latter is much greater than the oxygen content, which is caused by the continuous decrease of oxygen content during the graphitization process, in addition to the continuous increase of nitrogen content during the NH_3 activation process. Considering that a significant increase in nitrogen content may have a significant impact on the efficiency of electro-generating H_2O_2 , we have performed the peak separation processing on the N1s spectra of these two samples, including the following four peaks corresponding to nitrogen-containing groups [23,24] : Peak I (398.0-398.2 eV) corresponds to pyridinic nitrogen; Peak II (399.1-399.8 eV) corresponds to pyrrolic nitrogen; Peak III (400.2-400.9 eV) corresponds to graphitic nitrogen); Peak IV near 402.0 eV corresponds to other nitrogen oxide compounds. Fig. 3 shows the N1s peaks of PAN-CNFs and N-PAN-CNFs and their fitting curves. For PAN-CNFs, the pyridine nitrogen content (55%) is relatively high, while the graphite nitrogen is slightly lower than the pyrrole nitrogen content, and the total content of the two is about 40%. For N-PAN-CNFs, the pyridine nitrogen content (21%) is greatly reduced, but the graphite nitrogen content (38%) is greatly increased, meanwhile the pyrrole nitrogen content (24%) is also increased. It is to say, the significant increase in the nitrogen content in N-PAN-CNFs, is mainly attributed to the increase of the pyrrole nitrogen and graphite nitrogen, especially for the latter. This is mainly due to the cyclization of polyacrylonitrile during the graphitization and activation process, which makes the linear molecular chains of PAN form a trapezoidal structure, and the trapezoidal structure in the carbon fiber filament is cross-linked under a high temperature to form a two-dimensional graphite sheet [24]. And just such transformation further resulted in a drastic decrease in the relative content of pyridine nitrogen, meanwhile the graphite nitrogen and pyrrole nitrogen become the main nitrogen-containing functional groups. In other words, compared with PAN-CNFs, N-PAN-CNFs are rich in graphite nitrogen and pyrrole nitrogen (total content of 62%), and they may have a positive effect on the efficiency of electro-generating H_2O_2 [12,25].

In addition, the conductivity of the electrode is also an important factor that affects the efficiency of electro-generating H_2O_2 . In order to investigate the influence of the increase in nitrogen content on the conductivity of the electrode, we conducted a four-probe resistance test on PAN-CNFs and N-PAN-CNFs. It is found that the electrical conductivity of PAN-CNFs and N-PAN-CNFs is 61.6 and 93.7 S cm^{-1} , respectively, and the latter shows good electrical conductivity for two reasons: one is the high

degree of graphitization of carbon fiber filaments caused by graphitization, and the other maybe that the increase in graphite nitrogen content did not destroy the conductive network of graphite fibers.

In general, compared with PAN-CNFs, N-PAN-CNFs is an electro-Fenton cathode material that possesses a suitable pore structure, higher specific surface area, higher conductivity, more graphite nitrogen and pyrrole nitrogen.

3.2. Electrochemical measurements

In the above section, we conducted systematic characterizations on the physico-chemical properties of PAN-CNFs and N-PAN-CNFs, and here we carried out the electrochemical tests on their electro-generating H_2O_2 performance.



The ORR in acidic solution can be divided into two-electron pathway and 4-electron pathway, as shown in equation (6) and (7). The two-electron pathway can generate H_2O_2 , which is expected to occur in the electro-Fenton system. Fig. 4 is the electrochemical performance of electro-generating H_2O_2 for PAN-CNFs and N-PAN-CNFs in the blended $H_2SO_4+Na_2SO_4$ solution (pH=3). As shown in Fig. 4(a), the accumulation amount of H_2O_2 generated by PAN-CNFs increased rapidly with the increasing electrolysis time, and then slowly increased until it reached a stable state. However, during the same electrolysis time, the accumulation amount of H_2O_2 generated by N-PAN-CNFs basically rises at a constant rate. At the same time, the current efficiency of electro-generating H_2O_2 for PAN-CNFs decreases significantly greater than that of N-PAN-CNFs with the increasing electrolysis time, showing that N-PAN-CNFs has better electro-generation performance. In addition, we also investigated the cycle stability of electro-generated H_2O_2 for N-PAN-CNFs, as shown in Fig. 4(b). For the same N-PAN-CNFs electrode, we refreshed the solution after the electrolysis was completed, and then repeated the experiment. After 40 times, the accumulation amount of electro-generating H_2O_2 remained at about 89 mg L^{-1} , showing a good cycle stability.

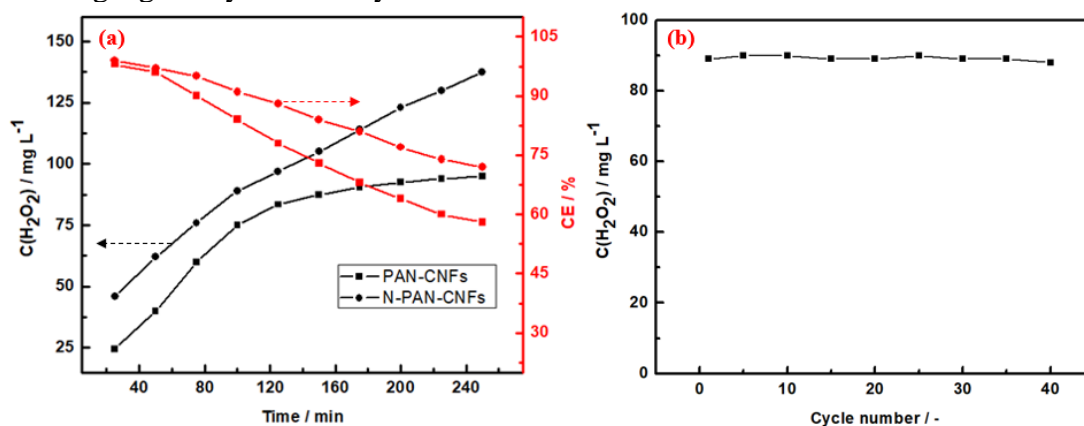


Figure 4. Electrochemical performance of the electro-generating H_2O_2 for PAN-CNFs and N-PAN-CNFs in the blended $H_2SO_4+Na_2SO_4$ solution with the pH of 3. (a) Changing curves of cumulative concentration of H_2O_2 and the corresponding CE with the electrolysis time; (b) Cycle performance curve of N-PAN-CNFs

In order to further study the electro-generating H_2O_2 performance, we first conducted the CV tests of PAN-CNFs and N-PAN-CNFs. Fig. 5(a) shows the CV curves of PAN-CNFs and N-PAN-CNFs in a $\text{H}_2\text{SO}_4+\text{Na}_2\text{SO}_4$ solution saturated with oxygen at pH 3, where the Na_2SO_4 concentration is 0.1 mol L^{-1} . Herein, the sweep rate is 10 mV s^{-1} , and the sweep potential range is 0-0.8 V. It can be seen that the upper part of the CV curve for PAN-CNFs and N-PAN-CNFs is approximately a rectangle, indicating that both of them exhibit a certain capacitance behavior [26], while the rectangular area of PAN-CNFs is significantly less than that of N-PAN-CNFs, meaning the latter has a larger surface area. In addition, both of them show a reduction peak corresponding to ORR at about 0.41 V, but the peak current of N-PAN-CNFs is significantly larger than that of PAN-CNFs. This is because, for one thing, the active surface area of the former is larger than that of the latter, for another, N-PAN-CNFs with rich graphite nitrogen and pyrrole nitrogen have better ORR electrocatalytic performance [12,25]. Although N-PAN-CNFs with good ORR activity have smaller activation polarization, the current response of N-PAN-CNFs is relatively large, consequently the ohmic potential drop produced by them is also relatively large. Therefore, its peak position in the CV curve is almost the same with that for PAN-CNFs.

Considering that N-PAN-CNFs have better ORR electrocatalytic performance, we conducted an in-depth mechanism research on the electrochemical performance of N-PAN-CNFs below. Firstly, we used the rotating disk electrode system to perform the LSV test in the above electrolyte. Herein, the sweep rate is 10 mV s^{-1} , the sweep potential range is 0-0.8 V, and the rotating speed is 400, 800, 1200, 1600 and 2000 rpm, respectively. Fig. 5(b) shows the LSV curves of N-PAN-CNFs at different rotate speeds. It can be seen that the initial onset potential of ORR is about 0.45 V, and its limiting diffusion current density increases with the increasing rotate speed.

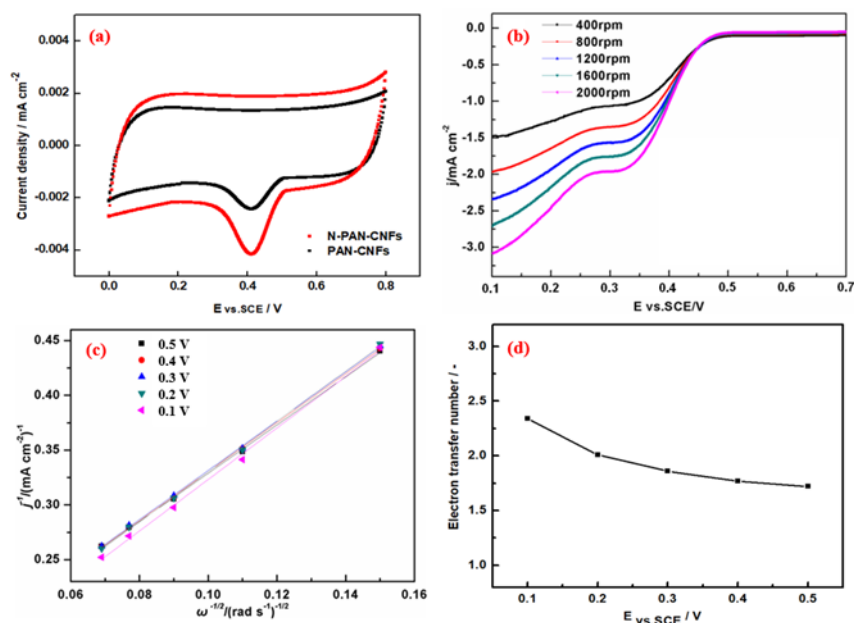


Figure 5. (a) CV curves of PAN-CNFs and N-PAN-CNFs in the blended $\text{H}_2\text{SO}_4+\text{Na}_2\text{SO}_4$ solution with the pH of 3; (b) LSV curves of N-PAN-CNFs with different rotate speed; (c) K-L curves of N-PAN-CNFs; (d) Electron transfer number for ORR on N-PAN-CNFs.

In addition, it is difficult to maintain the limiting diffusion current density of N-PAN-CNFs in a plateau state at a more negative potential, indicating that a continuous electron transfer reaction (2+2 electron reaction) may occurred at the surface of the electrode [27]. Generally speaking, the number of electron transfers participating in the ORR reaction can be obtained by the Koutecky-Levich (K-L) formula [28,29]:

$$j^{-1} = j_K^{-1} + j_L^{-1} = j_K^{-1} + (B\omega^{1/2})^{-1} \quad (8)$$

$$B = 0.62nFC_0(D_0)^{2/3}\nu^{-1/6} \quad (9)$$

Where j is the measured current density, j_K is the kinetic current density, j_L is the limiting diffusion current density, ω is the rotate speed of the electrode, n is the total number of electrons transferred in the ORR process, and C_0 is the initial concentration of oxygen in the electrolyte (about $2.5 \times 10^{-4} \text{ mol L}^{-1}$), D_0 is the diffusion coefficient of O_2 in $0.1 \text{ mol L}^{-1} \text{ Na}_2\text{SO}_4$ solution (about $1.4 \times 10^{-5} \text{ cm}^2 \text{ s}^{-1}$), ν is the dynamic viscosity of the electrolyte (about $0.01 \text{ cm}^2 \text{ s}^{-1}$) [30], other parameters are the same as described above.

Fig. 5(c) shows the K-L curve of N-PAN-CNFs in the electrolyte. It can be seen that j^{-1} and $\omega^{-1/2}$ show a good linear relationship during the potential range of 0.1-0.5 V. According to equation (8) and (9), the electron transfer number of ORR at different potentials can be obtained, as shown in Fig. 5(d). It can be seen that the electron transfer number of ORR at the surface of N-PAN-CNFs gradually increases with the negative shift of the scanning potential, but all of them are close to 2, and the average number of electron transfers is 2.05, indicating that the two-electron pathway is the main reaction process. With the further negative shift of the scanning potential, H_2O_2 may be further reduced to H_2O . In short, N-PAN-CNFs has a preferable electrocatalytic effect on the two-electron ORR and it is an excellent electro-generating H_2O_2 cathode material.

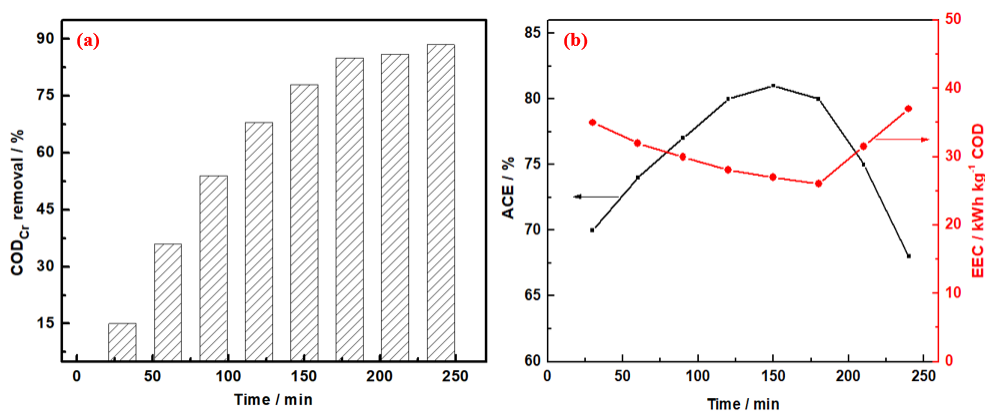


Figure 6. (a) Changing curves of COD_{Cr} removal with the electro-Fenton time; (b) Changing curves of ACE and EEC with the electro-Fenton time.

Moreover, there are a large amount of phenol and its derivatives in the industrial wastewater. Due to its high stability, high toxicity and high carcinogenic rate, it has caused serious damage to the ecological environment and brought a serious threat on the human health. So the pre-treatment of wastewater containing phenols is very important, and the treatment of phenolic pollutants using the

electro-Fenton technology has attracted widespread attention. Here we used a Na_2SO_4 solution (0.1 mol L^{-1}) containing 100 mg L^{-1} of phenol to simulate the industrial wastewater containing phenols, and used the N-PAN-CNFs as the electro-Fenton cathode material to degrade the phenolic pollutants. Fig. 6(a) shows the change curve of COD_{Cr} removal rate with the electrolysis time. It can be seen that with the increasing electro-Fenton time, the COD_{Cr} removal rate first increases rapidly and then increases slowly. The COD_{Cr} removal rate could reach 85% after 3 hours of electrolysis, while that could reach 88.5% after 4 hours. Fig. 6(b) shows the curves of ACE and EEC, which were obtained according to equations (4) and (5), with the electro-Fenton time. It can be seen that the ACE increases continuously in the first 150 mins, and then decreases rapidly, the highest value is 81.5%; while the corresponding EEC begins to decrease continuously, but gradually increases after 180 min, and the lowest value is 25.6 kWh kg^{-1} . Therefore, it can be concluded that N-PAN-CNFs is a highly-efficient electro-Fenton cathode material to degrade the phenolic pollutants.

4. CONCLUSIONS

In this work, we combined the electrospinning technology with following graphitization and activation treatment to achieve the construction of an electro-Fenton cathode material with suitable pore structure, high specific surface, good conductivity and electrochemical activity. Compared with PAN-CNFs, the fine particles on the surface of N-PAN-CNFs are significantly reduced, and more ravines are generated at the surface, consequently exhibiting a higher specific surface area ($89.7 \text{ m}^2 \text{ g}^{-1}$). In addition, there are mainly mesopores of about 4.5 and 7 nm distributed at the surface of N-PAN-CNFs, which is beneficial to improve the mass transfer process at the surface of the electrode. XPS analysis shows that N-PAN-CNFs have less oxygen content, but are rich in graphitic nitrogen and pyrrole nitrogen (total content of 62%). And the introduction of nitrogen functional groups, in addition to the graphitization treatment, make N-PAN-CNFs a good electrical conductivity. More importantly, the current efficiency of the electro-generated H_2O_2 for N-PAN-CNFs is as high as 98%, indicating an excellent electrochemical performance; meanwhile the current efficiency decreases slowly with the increasing electrolysis time, showing a good cycle stability. It is worth noting that N-PAN-CNFs have an excellent electrocatalytic effect on the two-electron ORR, which may be determined by the abundant graphite nitrogen and pyrrole nitrogen at the surface of the electrode. In addition, N-PAN-CNFs has a good degradation effect on the phenolic pollutants. The removal rate of COD_{Cr} and ACE after 3 hours of electrolysis with N-PAN-CNFs can reach 85% and 81.5%, respectively, while the corresponding EEC is only 25.6 kWh kg^{-1} . Therefore, N-PAN-CNFs is a highly-efficient electro-Fenton cathode material.

ACKNOWLEDGEMENTS

This work was supported by the Open project of State Key Laboratory of Heavy Oil Processing in China University of Petroleum (Y7F1911191).

References

1. G. S. Xia, Oxygen reduction reaction mechanism and electro-Fenton application of polyacrylonitrile-based carbon fiber cathode before and after modification, Qingdao: Ocean

- University of China, 2015.
- W. G. Barb, J. H. Baxendale, P. George and K. R. Hargrave, *Trans. Faraday Soc.*, 47 (1951) 462.
 - C. X. Yang, Application research on the Fenton and Electro-Fenton technology in organic wastewater treatment, Dalian: Dalian University of Technology, 2012.
 - Y. Wang, Y. H. Liu, T. F. Liu, S. Q. Song, X. C. Gui, H. Liu and P. Tsiakaras, *Appl. Catal. B-Environ.*, 156-157 (2014) 1.
 - I. Yamanaka, T. Onizawa, S. Takenaka and K. Otsuka, *Angew. Chem.-Int. Edit.*, 42 (2003) 3653.
 - J. Miao, H. Zhu, Y. Tang, Y. M. Chen and P. Y. Wan, *Chem. Eng. J.*, 250 (2014) 312.
 - L. Zhou, M. Zhou, Z. Hu, Z. Bi and K. G. Serrano, *Electrochim. Acta*, 140 (2014) 376.
 - P. Zhao, H. M. Zhang, H. T. Zhou, J. Chen, S. J. Gao and B. L. Yi, *J. Power Sources*, 162 (2006) 1416.
 - K. J. Kim, M. S. Park, Y. J. Kim, J. H. Kim, S. X. Dou and M. Skyllas-Kazacos, *J. Mater. Chem. A*, 3 (2015) 16913.
 - Y. H. Lee, F. Li, K. H. Chang, C. C. Hu and T. Ohsaka, *Appl. Catal. B-Environ.*, 126 (2012) 208.
 - X. Zhang, J. Fu, Y. Zhang and L. Lei, *Sep. Sci. Technol.*, 64 (2008) 116.
 - H. B. Xu, G. S. Xia, H. N. Liu, S. W. Xia and Y. H. Lu, *Phys. Chem. Chem. Phys.*, 17 (2015) 7701.
 - Z. X. Tai, X. B. Yan, J. W. Lang and Q. J. Xue, *J. Power Sources*, 199 (2000) 373.
 - C. Kim, K. S. Yang, M. Kojima, K. Yoshida, Y. Kim, Y. Kim and M. Endo, *Adv. Funct. Mater.*, 16 (2006) 2393.
 - G. J. Wei, X. Z. Fan, J. G. Liu and C. W. Yan, *J. Power sources* 270 (2014) 634.
 - G. J. Wei, X. Z. Fan, J. G. Liu and C. W. Yan, *J. Power sources*, 281 (2015) 1.
 - X. B. Zhang, M. H. Chen, X. G. Zhang and Q. W. Li, *Acta Phys. -Chim. Sin.*, 26 (2010) 3169.
 - G. J. Wei, J. G. Liu, H. Zhao, C. W. Yan, *J. Power Sources*, 241 (2013) 709.
 - R. M. Sellers, *Analyst*, 105 (1980) 950.
 - L. M. Zhen, Preparation of graphite-PTFE cathode and treatment of dye wastewater by electro-Fenton reaction, Qinquangdao: Yanshan University, 2010.
 - M. Zhou, Q. Tan, Q. Wang, Y. Jiao, N. Oturan and M. A. Oturan, *J. Hazard. Mater.*, 2012, 215 (2012) 287.
 - K. Wan, A. D. Tan, Z. P. Yu, Z. X. Liang, J. H. Piao and P. Tsiakaras, *Appl. Catal. B-Environ.*, 209 (2017) 447.
 - J. R. Pels, F. Kapteijn, J. A. Moulijn, Q. Zhu and K. M. Thomas, *Carbon*, 33 (1995) 1641.
 - C. Weidenthaler, A.-H. Lu, W. Schmidt and F. Schüth, *Microporous Mesoporous Mater.*, 88 (2006) 238.
 - X. Z. Fan, Y. H. Lu, H. B. Xu, X. F. Kong and J. Wang, *J. Mater. Chem.*, 21 (2011) 18753.
 - H. Niwa, K. Horiba, Y. Harada, M. Oshima, T. Ikeda, K. Terakura, J.-I. Ozaki and S. Miyata, *J. Power Sources*, 187 (2009) 93.
 - D. H. Guo, R. Shibuya, C. Akiba, S. Saji, T. Kondo and J. Nakamura, *Science*, 351 (2016) 361.
 - N. Alexeyeva, E. Shulga, V. Kisand, I. Kink and K. Tammeveski, *J. Electroanal. Chem.*, 2010, 648 (2010) 169.
 - M. Vikkisk, I. Kruusenberg, U. Joost, E. Shulga and K. Tammeveski, *Electrochim. Acta*, 87 (2013) 709.
 - B. Garza-Campos, D. Morales-Acosta, A. Hernández-Ramírez, J. L. Guzmán-Mar, L. Hinojosa-Reyes, J. Manríquez and E. J. Ruiz-Ruiz, *Electrochim. Acta*, 269 (2018) 232.